

*Research Article*

## A Spatially Extended Model for Residential Segregation

Antonio Aguilera and Edgardo Ugalde

Received 15 August 2006; Accepted 5 March 2007

We analyze urban spatial segregation phenomenon in terms of the income distribution over a population, and an inflationary parameter weighting the evolution of housing prices. For this, we develop a discrete spatially extended model based on a multiagent approach. In our model, the mobility of socioeconomic agents is driven only by the housing prices. Agents exchange location in order to fit their status to the cost of their housing. On the other hand, the price of a particular house depends on the status of its tenant, and on the neighborhood mean lodging cost weighted by a control parameter. The agent's dynamics converges to a spatially organized configuration, whose regularity is measured by using an entropy-like indicator. This simple model provides a dynamical process organizing the virtual city, in a way that the population inequality and the inflationary parameter determine the degree of residential segregation in the final stage of the process, in agreement with the segregation-inequality thesis put forward by Douglas Massey.

Copyright © 2007 A. Aguilera and E. Ugalde. This is an open access article distributed under the Creative Commons Attribution License, which permits unrestricted use, distribution, and reproduction in any medium, provided the original work is properly cited.

### 1. Introduction

The spatial structure of a city is the result of a wide and complex set of factors. The way in which different economic activities and social groups spread over the urban space is the matter of different and complementary theories in sociology, geography, politics, and economy [1–4]. Housing patterns can be understood as the result of the complex interrelationship between individuals' actions constrained by social, political, and economical rules [2, 5]. Residential segregation is the degree to which two or more groups live separately from one to another in different parts of the urban space [6, page 282]. This phenomenon is concurrent to several social problems as the concentration of low opportunities to get a well-earned job, low scholar development in children of segregated

## 2 Discrete Dynamics in Nature and Society

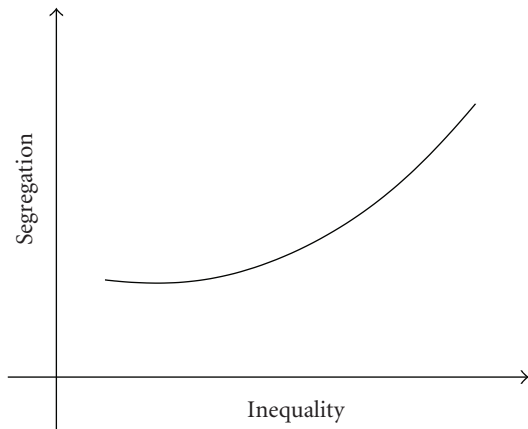


Figure 1.1. Segregation-inequality curve according to Morrison et al. [28].

areas, premature parenthood between young people, and the emergence of criminality [7, 8].

Residential segregation has been the subject of extensive research in social sciences for many years. It is a multifactorial phenomenon mainly determined by socioeconomic factors like race and income distribution, as well as factors associated to the structure of the urban space [7–11].

There are two main quantitative approaches to segregation, the phenomenological one which relies on segregation measures and indexes [6, 12, 13], and the theoretical one based on computational or mathematical models [7, 8, 11, 14–27].

In this paper we propose a spatially extended model based on ideas of Portugal et al. [23] and Schelling [24–26] to explore, in a mathematical and computational way, the relationship between two social variables: the income inequality and the residential segregation. Our interest in this relationship is motivated by a thesis formulated by Massey et al. [7], which establishes that the degree of spatial segregation experienced by a society increases with its level of inequality. This relationship has been formulated in a graphical way by Morrison et al. [28] as the segregation-inequality curve (see Figure 1.1).

As many other phenomena studied by socioeconomic sciences (e.g., price formation [29], opinion formation and voting [30–33], belief and rumor propagation [34–36], formation of cultural domains [37, 38]), residential segregation has motivated the curiosity of researchers in the area of dynamical systems [39, 40]. Our work should be primarily understood as a contribution to the study of a discrete dynamical systems inspired by socioeconomic phenomena. It can also be placed inside a tradition started by social scientists as Schelling [24–26] and Sakoda [41], and followed by Clark [15], Fosset [16, 17], Osullivan et al. [22], and Zhang [27], who used mathematical models to study the underlying mechanisms in social processes.

The organization of the paper is as follows. In the next section we briefly expose the main theoretical studies concerning the residential segregation, emphasizing only the

ideas and concepts that are relevant to our research. In Section 3 we present the mathematical model and the tools needed to analyze our numerical simulation, which we do in Section 5. Previous to this, in Section 4 we study asymptotic behavior of the model, and derive some theoretical estimates which we consider for the numerical study. Finally, we conclude with a discussion about the potential of our model as vehicle for the exploration of the role of income inequality in residential segregation phenomena.

## 2. The segregated city

Residential segregation is a complex phenomenon with several dimensions of analysis, whose governing mechanisms are hard to identify. In a first approximation, we can however assume that the phenomenon is governed by a set of structural and behavioral rules which determine the possibility of one individual to get a particular kind of house in a specific location of the city. Since those rules are not evident, simplifying hypotheses are required.

One point of view, based on human ecology, postulates that residential segregation occurs because individuals in a city are in mutual competition for the space and its resources. According to this approach, competition is the main force driving the residential segregation [2, page 86]. The outcome of this competition is determined by the ability of individuals to struggle for advantageous locations in the urban space, that is, their dominant capacity, which is constrained by sociocultural and socioeconomic rules [2, pages 85–88].

There are three main hypotheses about the sociocultural rules governing the residential segregation. The first one concerns the class-selective emigration from poor regions. In a region where both poor and less poor people coexist, the latter tend to emigrate to a more wealthy region. This mechanism tends to isolate and concentrate poor people, increasing in this way the poverty rate of the region. The second hypothesis establishes that neighborhood concentration of poor people reflects the general poverty of the urban area. When the average shows a downward trend, neighborhood poverty rates increase. Finally, the third is related to the racial segregation experienced by poor people. Racial bias causes racial segmentation of the urban housing markets, which concurs with high rates of poverty in specific ethnic groups to concentrate poverty geographically (see [8, pages 426–428], and references therein). These hypotheses are complementary, and were developed to explain segregation in North-American cities, where they have been tested. Perhaps in the Latino-American case, racial and sociocultural factors have a less relevant role, making it possible to build an explicative model over socioeconomic considerations only.

Taking into account that “markets are not mere meetings between producers and consumers, whose relations are ordered by the interpersonal laws of supply and demand” [3, page 1], we can formulate socioeconomic rules as market mechanisms. The housing market is formed by two kinds of agents: residents which are interested in the social and individual value or use of the land commodity, and the entrepreneurs which are interested in the exchange value of the land. There is a natural conflict between these two of valuations of land.

## 4 Discrete Dynamics in Nature and Society

There is a set of structural factors that are relevant to housing market dynamics: (a) the housebuilding industry; (b) the government's housing policy; (c) the structure of the property of land; (d) the actual spatial structure of city, that is, location of labor area, residential areas, and trade-commerce areas; and (e) the income structure of the society. The last one has been considered as the most significant for the residential segregation phenomenon. Indeed, urban economic theory explains the formation of segregated cities through two main arguments. The first one establishes that a population of households with heterogeneous income competing for the occupation of urban land traditionally results in an income-based stratification of the urban space according to the distance to the city center [42]. The second one links the concentration of low incomes households in some areas to the existence of local externalities like ethnicity. As a consequence of this, there is a households' preference to live in relative homogeneous neighborhoods with respect to either income or ethnic similarity [26, 43, 44].

Two levels of analyses may be considered in the study of residential segregation. At the macro level, several structural transformations in the society (changes in income level, tendency to racial exclusion, levels of social integration, etc.) are assumed to determine the spatial concentration of poverty. This is the level of analysis in [8–10, 45]. At the microlevel, specific discriminatory individual behaviors related individual characteristics (sex, age, religion, ethnic group, nationality, etc.) influence the choice of a place to live. This is the point of view in [15, 23–26, 46], and it is also the one we adopt here.

Our model was developed with the purpose of studying Massey et al.'s thesis [7, page 400], which relates the degree of spatial segregation experienced by a society to its inequality degree (income disparity). This thesis was reformulated as the segregation-inequality curve (see Figure 1.1) by Morrison et al. [28]. More precisely, we intend to determine the relationship between these two quantifiable phenomena, inequality, and segregation, in a situation where the whole dynamics is governed by basic rules of socioeconomic nature.

### 3. Model structure

Our model is inspired in the works of Schelling [24, 25] and Portugali et al. [23]. Like Portugal's models, the physical infrastructure of our "simplified city" is modeled by a two-dimensional lattice of finite size  $\Lambda_n = \{1, 2, \dots, n\} \times \{1, 2, \dots, n\}$ . A two-dimensional integer vector  $\mathbf{x} = (\mathbf{x}_1, \mathbf{x}_2) \in \Lambda_n$  represent spatial coordinates. At each time step, the prices of the house at location  $\mathbf{x}$  is a positive real number, originally in the interval  $[0, 1]$ . Each house is occupied by a householder or agent, who can be distinguished only by his/her socioeconomic status. We quantify this status with a real number taking one of three possible values  $p < m < r$  (which stands for poor, middle class, and rich, resp.) in the interval  $[0, 1]$ . Houses are identical in their characteristics but differentiable by their prices.

There are two main mechanism setting up the house's prices dynamics: the neighborhood influence and the householder's economic status. On the other hand, the agents change position subject to availability, under the pressure of their housing situation. Agents can move inside the city to achieve an optimal match between their status and the price of the house they inhabit. Agents try to live in houses with prices suiting their economic status.

At time  $t$ , the prices of houses are encoded in an  $n \times n$  matrix  $V^t := (V^t(\mathbf{x}))_{\mathbf{x} \in \Lambda_n}$ , while the spatial distribution of agents is stored in a numerical  $n \times n$  matrix  $A^t := (A^t(\mathbf{x}))_{\mathbf{x} \in \Lambda_n}$  with values in  $\{p, m, r\} \subset [0, 1]$ . This means that at time  $t$ , the value of the house at location  $\mathbf{x}$  is  $V^t(\mathbf{x})$ , and the status of the agent living in that location is quantified by the number  $A^t(\mathbf{x})$ , which in our numerical experiments takes values  $r = 1$ ,  $m = 1/2$ , or  $p = 1/10$ . The price of the house at location  $\mathbf{x}$  evolves, from time  $t$  to  $t+1$ , according to

$$V^{t+1}(\mathbf{x}) = A^{t+1}(\mathbf{x}) + \lambda \frac{\sum_{\mathbf{y} \in \mathcal{N}(\mathbf{x})} V^t(\mathbf{y})}{\#\mathcal{N}(\mathbf{x})}, \quad (3.1)$$

where  $\mathcal{N}(\mathbf{x}) := \{\mathbf{y} \in \Lambda_n : |\mathbf{x}_1 - \mathbf{y}_1| + |\mathbf{x}_2 - \mathbf{y}_2| \leq 2\}$  is the square neighborhood of radius 2 centered at  $\mathbf{x}$ . If  $\mathbf{x}$  is located far from the boundaries of the lattice,  $\#\mathcal{N}(\mathbf{x}) = 25$ . This cardinality diminishes as  $\mathbf{x}$  approaches the boundaries. The parameter  $\lambda$  weights the influence of the mean price on the neighborhood over the house price, and can be thought as an inflationary parameter: the larger  $\lambda$  is the higher the asymptotic mean value of the houses in the city is.

After updating the values of houses, the agents are relocated according to the following rule. We randomly select two locations  $\mathbf{x}, \mathbf{y} \in \Lambda_n$  and try to exchange the agents at these locations. This would correspond to replace  $A^t(\mathbf{x})$  by  $A^t(\mathbf{y})$  and *vice versa*. In order to decide whether this relocation is retained or not, we compare the new distribution of agents with the spatial distribution of house prices. For this, we define

$$\delta(\mathbf{x}, \mathbf{y}) := (A^t(\mathbf{x}) - V^t(\mathbf{x}))^2 - (A^t(\mathbf{y}) - V^t(\mathbf{x}))^2 + (A^t(\mathbf{y}) - V^t(\mathbf{y}))^2 - (A^t(\mathbf{x}) - V^t(\mathbf{y}))^2. \quad (3.2)$$

This quantifies the economic improvement due to the attempted house exchange between agents at locations  $\mathbf{x}$  and  $\mathbf{y}$ . Notice that each time, only two agents are considered for a house exchange. This relocation takes place only if  $\delta(\mathbf{x}, \mathbf{y}) > 0$ , that is, if the exchange gives place to an economic improvement for the agents involved. Summarizing, at time  $t$  we select two locations  $\mathbf{x}, \mathbf{y} \in \Lambda_n$ , and update  $A^t$  as follows:  $A^{t+1}(\mathbf{z}) = A^t(\mathbf{z})$  for  $\mathbf{z} \notin \{\mathbf{x}, \mathbf{y}\}$ , and

$$\begin{aligned} \text{if } \delta(\mathbf{x}, \mathbf{y}) > 0 &\quad \text{then } A^{t+1}(\mathbf{x}) = A^t(\mathbf{y}), \quad A^{t+1}(\mathbf{y}) = A^t(\mathbf{x}), \\ \text{else } &\quad A^{t+1}(\mathbf{x}) = A^t(\mathbf{x}), \quad A^{t+1}(\mathbf{y}) = A^t(\mathbf{y}). \end{aligned} \quad (3.3)$$

The economic improvement due to a house exchange leads to the reduction on the economic tension

$$T(A, V) = |A - V| := \sqrt{\sum_{\mathbf{x} \in \Lambda_n} (A(\mathbf{x}) - V(\mathbf{x}))^2}. \quad (3.4)$$

Agents try to minimize the economic tension generated by difference between housing price and status. In our model, this difference plays the same role as the dissatisfaction or the unhappiness in Schelling's model [24–26]. Notice that the evolution of agents' distribution in space satisfies an exclusion principle, according to which two agents cannot occupy the same location.

## 6 Discrete Dynamics in Nature and Society

**3.1. Analytical tools.** The segregation-inequality curve gives the relation between two characteristics of the system: inequality and segregation. The income distribution can be interpreted as a probability vector. The proportions of the population in each income group would be the probability for an individual to belong to that income group. With this idea, income inequality can be measured by using Theil's inequality index [47, pages 91–96]. Adapting this index to our situation, we define inequality of an  $n \times n$  agents' distribution  $A$  as follows:

$$I(A) = \log(3) + \sum_{i=p,m,r} q_i \log(q_i), \quad (3.5)$$

where for  $i = p, m, r$ ,  $q_i = \#\{\mathbf{x} \in \Lambda_n : A(\mathbf{x}) = i\}/n^2$  is the proportion of agents in each income group. The inequality so defined is an entropy-like indicator taking values in the interval  $[0, \log(3)]$ . The minimum  $I$  corresponds to the case where the total population is equally distributed among all the income groups, and maximum to the limit case of a single income group concentrating in the whole population. This last limit would be obtained from distributions where a given income group includes most of the population.

The other characteristic we need to determine the segregation curve is the spatial segregation itself. Though measures of segregation have been the subject of several works in sociology (see [19, page 283] and references therein), it is more suitable to our approach to quantify this characteristic by using the degree of order of a given spatial distribution. The idea is to associate the maximum degree of order to a spatial distribution which can be easily described, like a single cluster or a periodic distribution. On the other hand, a random distribution would have a low degree of order. We use an image segmentation technique, the biorthogonal decomposition to associate a degree of disorder (the entropy of the biorthogonal decomposition), to a given spatial distribution which we treat as an image [48, page 131]. Thus, to quantify the segregation (ordering) of the city, we compare the entropy of the biorthogonal decomposition of the ordered distribution with that corresponding to a random distribution.

The biorthogonal decomposition is the bidimensional generalization of the Karhunen-Loëve transform, but with the advantage that it is sensible to changes in the spatial structure of one image. To a biorthogonal decomposition an entropy is associated, which measures the amount of information of the image [48, page 133]. A spatial pattern corresponds to an inhomogeneous distribution of pixels and this kind of images has low entropy, while absence of a spatial pattern corresponds to a random distribution of pixels, which has the highest entropy.

Consider an  $n \times n$  positive matrix  $U$ , which is supposed to codify an image or a two-dimensional distribution. The associate covariance matrix  $Q := U^\dagger U$  is symmetric, and hence its eigenvalues  $\{\lambda_i : i = 1, \dots, n\}$  are real, and the corresponding eigenvectors  $\{\phi_i : i = 1, \dots, n\}$  define an orthonormal basis. The biorthogonal decomposition allows us to rewrite the matrix  $U$  as

$$U = \sum_{i=1}^m \psi_i \phi_i^\dagger, \quad (3.6)$$

where  $\psi_i = U\phi_i$  for  $i = 1, 2, \dots, n$ . The contribution of the submatrix  $\psi_i\phi_i^\dagger$  to the sum is of the order of the corresponding eigenvalue  $|\lambda_i|$ . The information of the matrix  $U$  is concentrated in the submatrices associated to eigenvalues with the highest absolute value. For positive  $U$ , we neglect the largest eigenvalue  $\lambda_1$ , which can be associated to a spatially homogeneous mode. Using the eigenvalue structure of the biorthogonal decomposition, we define the information contents of  $U$  by

$$H_{\text{BO}}(U) = - \sum_{i=2}^n p_i \ln p_i, \quad (3.7)$$

where

$$p_i = \frac{|\lambda_i|}{\sum_{k=2}^n |\lambda_k|}. \quad (3.8)$$

For an agent distribution  $A$ , the segregation index is

$$S_{\text{BO}}(A) = \mathbb{E}(H_{\text{BO}}) - H_{\text{BO}}(A), \quad (3.9)$$

where  $\mathbb{E}(H_{\text{BO}})$  is the expected value of  $H_{\text{BO}}$  with respect to a random distribution of agents in the  $(n \times n)$ -dimensional lattice. We have numerically found that  $\mathbb{E}(H_{\text{BO}}) \approx \log(3/5 \times n)$  for  $n \leq 1000$ .

#### 4. Asymptotic behavior of the model

In order to understand the asymptotic behavior of the model, let us rewrite (3.1) and (3.3) in matrix form as follows:

$$\begin{aligned} V^{t+1} &= A^t + \lambda D V^t, \\ A^{t+1} &= P^t A^t, \end{aligned} \quad (4.1)$$

where both  $V^t$  and  $A^t$  have to be considered as  $(m \times n)$ -dimensional vectors,  $D$  is the averaging matrix whose action is defined by (3.1), and  $P^t$  is a permutation matrix which permutes at most two coordinates. If for the chosen coordinates  $\mathbf{x}, \mathbf{y} \in \Lambda_n$  we have  $\delta(\mathbf{x}, \mathbf{y}) > 0$ , then  $P^t$  is the matrix permuting those coordinates, otherwise  $P^t$  is the identity matrix.

After a sufficiently large number of iterations, named  $T$ , the agents achieve a spatial distribution  $A^*$  which cannot be improved. From that point on, the distribution of housing prices follows the affine evolution  $V^{T+t} = A^* + \lambda D V^{T+t-1}$ , so that

$$V^{T+t} = (\lambda D)^t V^T + \left( \sum_{s=0}^{t-1} (\lambda D)^s \right) A^* = (\lambda D)^t V^T + (\text{Id} - (\lambda D)^t)(\text{Id} - \lambda D)^{-1} A^*. \quad (4.2)$$

The long-term distribution of housing prices is therefore  $V^* := (\text{Id} - \lambda D)^{-1} A^*$ , so that the economic tension associated to the asymptotic distribution of agents is

$$T^*(A^*) := T(A^*, V^*) = |A^* - (\text{Id} - \lambda D)^{-1} A^*| = \lambda \times |(\text{Id} - \lambda D)^{-1} (D A^*)|. \quad (4.3)$$

## 8 Discrete Dynamics in Nature and Society

Because of the nondeterministic nature of the evolution of our system, the asymptotic distribution  $A^*$  is not uniquely determined by initial conditions. Nevertheless, it has to satisfy the following “variational principle”:

$$T^*(A^*) = \min_P |(P - (\text{Id} - \lambda D)^{-1})A^*|, \quad (4.4)$$

where the minimum is taken over the set of all two-sites permutations. This is equivalent to say that asymptotically no location exchange can diminish the economic tension.

**4.1. Critical  $\lambda$ .** For  $\lambda$  small, a spatially disordered initial distribution of agents  $A^0$  remains unchanged, and the system evolves following an affine law, converging to  $A^* = A^0$ ,  $V^* = (\text{Id} - \lambda D)^{-1}A^0$ . For each spatially disordered initial distribution  $A^0$ , there exists a critical value  $\lambda_c$  for which  $A^0$  evolves towards a spatially organized state  $A^*$ . This distribution is composed by relatively small number of clusters, each one of them consisting of a nucleus of rich agents surrounded by middle class ones, while the lower-class agents occupy the space left by the clusters. In our numerical experiments, which we describe below, we have found that  $\lambda_c$  essentially depends on the proportion of  $r$ ,  $m$ , and  $p$  in  $A^0$ .

A two-sites permutation  $A^* \mapsto PA^*$  produces a change in the economic tension,

$$T^*(A^*) \mapsto |\lambda(\text{Id} - \lambda D)^{-1}(DA^*) + (A^* - PA^*)|. \quad (4.5)$$

According to (4.4), this change does not make the economic tension decrease. In order for this to be so, it is necessary that

$$|PA^* - A^*|^2 \geq 2\lambda((\text{Id} - \lambda D)^{-1}(DA), PA^* - A^*), \quad (4.6)$$

for each two-sites permutation  $A^* \mapsto PA^*$ . We may decompose  $DA^* = \overline{A^*}\mathbf{1} + f$  as the sum of a constant vector and a fluctuating one. Since

$$(\text{Id} - \lambda D)^{-1}\mathbf{1} = \frac{\mathbf{1}}{1 - \lambda} \quad (4.7)$$

and  $(\mathbf{1}, PA^* - A^*) = 0$ , then (4.6) can be written as

$$|PA^* - A^*|^2 \geq 2\lambda((\text{Id} - \lambda D)^{-1}f, PA^* - A^*). \quad (4.8)$$

Taking this into account, we may define  $\lambda_c$  as

$$\lambda_c = \min \left\{ \lambda > 0 : \frac{1}{2} < \max_P \frac{\lambda((\text{Id} - \lambda D)^{-1}f, PA^* - A^*)}{|PA^* - A^*|^2} \right\}, \quad (4.9)$$

where the maximum is taken over the two-sites permutations. For  $P$  interchange coordinates  $\mathbf{x}$ ,  $\mathbf{y}$ , we have

$$\frac{\lambda((\text{Id} - \lambda D)^{-1}f, PA^* - A^*)}{|PA^* - A^*|^2} \equiv \frac{((\text{Id} - \lambda D)^{-1}f)_x - ((\text{Id} - \lambda D)^{-1}f)_y}{2(A_y^* - A_x^*)}. \quad (4.10)$$

**4.2. An a priori estimate for  $\lambda_c$ .** A reasonably good estimate for  $\lambda_c$  can be obtained as follows. Considering  $A^*$  as a random field, the central limit theorem ensures that with very high probability,  $DA_x^* \in [\bar{A}^* - 2\tilde{\sigma}, \bar{A}^* + 2\tilde{\sigma}]$ , where

$$\tilde{\sigma} = \frac{1}{\sqrt{N}} \sqrt{\mathbb{E}((A_x^* - \bar{A}^*)^2)} \quad (4.11)$$

Here  $N$  is the number of sites in the computation of the local mean  $DA_x^*$ , which in our case is 25. Hence, with very high probability,

$$\max_{x,y} |f_x - f_y| = 4\tilde{\sigma} = \frac{4}{5} \sqrt{\rho_r(r - \bar{A}^*)^2 + \rho_m(m - \bar{A}^*)^2 + \rho_p(p - \bar{A}^*)^2}, \quad (4.12)$$

where  $\rho_r, \rho_m, \rho_p$  are the proportions of  $r, m$  and  $p$  in  $A^*$ , respectively. By using the upper bound

$$\max_{x,y} |((\text{Id} - \lambda D)^{-1} f)_x - ((\text{Id} - \lambda D)^{-1} f)_y| \lesssim \frac{\max_{x,y} |f_x - f_y|}{1 - \lambda}, \quad (4.13)$$

we obtain

$$\begin{aligned} \max_P \frac{\lambda((\text{Id} - \lambda D)^{-1} f, PA^* - A^*)}{|PA^* - A^*|^2} \\ \lesssim \frac{\lambda}{1 - \lambda} \times \frac{2\sqrt{\rho_r(r - \bar{A}^*)^2 + \rho_m(m - \bar{A}^*)^2 + \rho_p(p - \bar{A}^*)^2}}{5(m - p)}. \end{aligned} \quad (4.14)$$

According to (4.9), for  $\lambda \geq \lambda_c$ , we have

$$\frac{1}{2} < \frac{\lambda}{1 - \lambda} \times \frac{2\sqrt{\rho_r(r - \bar{A}^*)^2 + \rho_m(m - \bar{A}^*)^2 + \rho_p(p - \bar{A}^*)^2}}{5(m - p)}. \quad (4.15)$$

Taking this into account, we propose

$$\lambda^* := \frac{5(m - p)}{4\sqrt{\rho_r(r - \bar{A}^*)^2 + \rho_m(m - \bar{A}^*)^2 + \rho_p(p - \bar{A}^*)^2} + 5(m - p)} \quad (4.16)$$

as an estimate for  $\lambda_c$ .

**4.3. An a priori estimate for  $S_{BO}(A^*)$  at  $\lambda_c$ .** Suppose that  $A^*$  is composed by  $N_c$  clusters of comparable size, and suppose also that all of them are symmetric with respect to the coordinate axes. In this case,  $A^*$  has a cluster decomposition

$$A^* := \sum_{i=1}^{N_c} Q_i P_i^\dagger, \quad (4.17)$$

where  $Q_i P_i^\dagger$  corresponds to the  $i$ th cluster. The vectors  $P_i$  and  $Q_i$  have a belled form with maximal value at coordinates where the cluster is located. The vectors  $\{P_i\}_{i=1}^{N_c}$  span a

vector space of dimension  $n_c \leq N_c$ , for which  $\{p_k\}_{k=1}^{n_c}$  is an orthonormal basis obtained from  $\{P_i\}_{i=1}^{N_c}$  by the Gram-Schmidt process. Using this orthonormal base, we can rewrite  $A^* := \sum_{k=1}^{n_c} q_k p_k^\dagger$ , where the vectors  $q_k$  are obtained from  $Q_i$  after the change of basis. With respect to this new basis,  $A^*$  can be considered a random  $n_c$ -dimensional matrix, therefore  $H_{\text{BO}}(A^*) \approx \log(2 * n_c/3)$ , and hence

$$S_{\text{BO}}(A^*) \approx \log\left(\frac{n}{n_c}\right). \quad (4.18)$$

Let  $N_{\min}$  be the cardinality of the less numerous class of agents, that is,

$$N_{\min} = \min_{i=p,m,r} \#\{\mathbf{x} \in \Lambda_n : A^*(\mathbf{x}) = i\}. \quad (4.19)$$

For small values of the inequality index, that is, for large  $N_{\min}$ , we have numerically found that  $n_c \approx \sqrt{N_{\min}}$ . This is consistent with an agents' distribution  $A^*$  formed by  $N_c \propto N_{\min}$  clusters, each cluster containing nearly the same number of agents of the less numerous class. The corresponding cluster decomposition would be obtained from a collection  $\{Q_i\}_{i=1}^{n_1}$  of  $n_1 \propto \sqrt{N_{\min}}$  bell-shaped vectors, and another collection  $\{P_j\}_{j=1}^{n_2}$  of  $n_2 \approx \sqrt{N_{\min}}$  nearly orthonormal bell-shaped vectors as

$$A^* = \sum_{i=1}^{n_1} \sum_{j=1}^{n_2} Q_i P_j^\dagger. \quad (4.20)$$

In this case, we have  $N_c = n_1 \times n_2 \propto N_{\min}$ , and  $n_c = n_2 \approx \sqrt{N_{\min}}$ . Hence, for low values of the inequality index  $I$ , we may expect

$$S_{\text{BO}}(A^*) \approx S^* := \log\left(\frac{n}{\sqrt{N_{\min}}}\right). \quad (4.21)$$

Note that  $N_{\min}$  does not determine the value of  $I$ . If this value is large enough, the variability of  $N_{\min}$  inside the collection of agents' distributions with the same  $I$  value produces a large dispersion in  $S^*$ . For this reason, it is not possible to define  $S^*$  as a function of  $I$ , therefore an only inequality-segregation curve does not exist.

## 5. Numerical results

We performed a set of numerical experiments in the  $n \times n$  lattice, for  $n = 64$  and  $128$ . Each lattice node represents a house location in our virtual city, where agents and values of houses are distributed. At time  $t$ , these distributions are codified by  $n \times n$  real-valued matrices. The agent's matrix  $A^t$  takes only three values,  $r = 1$ ,  $m = 1/2$ , and  $p = 1/10$ , representing the income of rich, middle class, and poor agents, respectively. The distribution of house prices  $V^t$  is a positive matrix, which at time  $t = 0$  takes values in the interval  $[0, 1]$ . Both spatial distributions  $V^t$  and  $A^t$  evolve interrelatedly according to (3.1) and (3.3). The unevenness of an agent's distribution  $A$  is measured by using Theil's index  $I(A)$  defined in (3.5). Since this indicator depends only on the proportions of rich, middle class, and poor agents, then  $I(A^t) = I(A^0)$  for all  $t \geq 0$ .

Modeling the demographic composition of a city in a developing country, we have considered “demographic scenarios,” each demographic scenario consisting of a given number  $N_p$  of poor agents,  $N_m$  of middle class agents, and  $N_r$  of rich agents, such that  $N_r < N_m < N_p$ . In order to obtain an inequality-segregation curve, we have chosen two distinct one-parameter families of demographic scenarios. For the first family,  $N_p$  increases from half to the total population, while the ratio  $\alpha = N_r/N_m < 1$  is kept constant. In this way, we obtain the family

$$\mathcal{F}_\alpha := \left\{ (N_p, N_m, N_r) \simeq (\eta n^2, (1-\alpha)(1-\eta)n^2, \alpha(1-\eta)n^2) : \frac{1}{2} < \eta \right\}, \quad (5.1)$$

which we call “regular.” The second family of demographic scenarios is obtained as follows. We provide the set of all possible demographic scenarios with a probability distribution  $\mathbb{P}$  such that

$$\mathbb{P}(N_r, N_m, N_p) \propto \# \left\{ (n_1, n_2, n_3), 1 \leq n_i < n^2 : \frac{N_r}{n_1} = \frac{N_m}{n_2} = \frac{N_p}{n_3} \right\}. \quad (5.2)$$

This is the probability for three random numbers in  $\{1, 2, \dots, n^2\}$  to be proportional to the three given populations  $N_r$ ,  $N_m$  and  $N_p$ . For each value of  $I \in [0, \log(3)]$ , we choose the demographic scenario maximizing  $\mathbb{P}$  among all the demographic scenarios with inequality index  $I$ . In this way, we obtain a family  $\mathcal{F}_{mp}$  of demographic scenarios which we call “most probable.”

For both, the regular family and the family of most probable scenarios, we have considered equally spaced values of  $\lambda$  and  $I$  inside an appropriated region of the parameter space. In the case of the regular family  $\mathcal{F}_\alpha$ , the minimum inequality index  $I_\alpha := \log(3) + 1/2 \log(1/2) + \alpha/2 \log(\alpha/2) + (1-\alpha)/2 \log((1-\alpha)/2)$  depends on  $\alpha$ , while for the family of most probable scenarios, all inequality indices in  $[0, \log(3)]$  are possible. For the regular family, we consider 10 demographic scenarios with inequality indices

$$I = I_\alpha, I_\alpha + \frac{\log(3) - I_\alpha}{9}, I_\alpha + \frac{2(\log(3) - I_\alpha)}{9}, \dots, I_\alpha + \frac{9(\log(3) - I_\alpha)}{9}, \quad (5.3)$$

and for each one of those values we take  $\lambda = \lambda^* - 0.1, \lambda^* - 0.05, \lambda^*, \lambda^* + 0.05, \lambda^* + 0.1$ . In the case of the family of most probable scenarios, we consider 9 demographic scenarios with inequality indices  $I = 0, \log(3)/8, \log(3)/4, \dots, \log(3)$ , and again for each one of those values, we take  $\lambda = \lambda^* - 0.1, \lambda^* - 0.05, \lambda^*, \lambda^* + 0.05, \lambda^* + 0.1$ . Since our theoretical estimation  $\lambda^*$  depends on  $I$ , the region of parameters we studied is not rectangular. For each  $I$  and  $\lambda$  in the chosen region, we performed 20 experiments for both the  $64 \times 64$  and the  $128 \times 128$  lattices. The purpose of these experiments was (1) to determine  $\lambda_c$  and compare it to our estimate; (2) to compute the value of the segregation index at  $\lambda = \lambda_c$ . This allowed us to draw the segregation-inequality curve.

Each experiment started with spatial distributions  $V^0$  and  $A^0$  randomly generated. The entries of  $V^0$  were always taken independently and uniformly distributed in the interval  $[0, 1]$ , while for  $A^0$  the agents determining a given demographic scenario were randomly distributed in the lattice. The experiment consisted in the iteration of the evolution rule, (3.1) and (3.3), until a stationary distribution  $A^*$  was reached. In Figure 5.1, we show

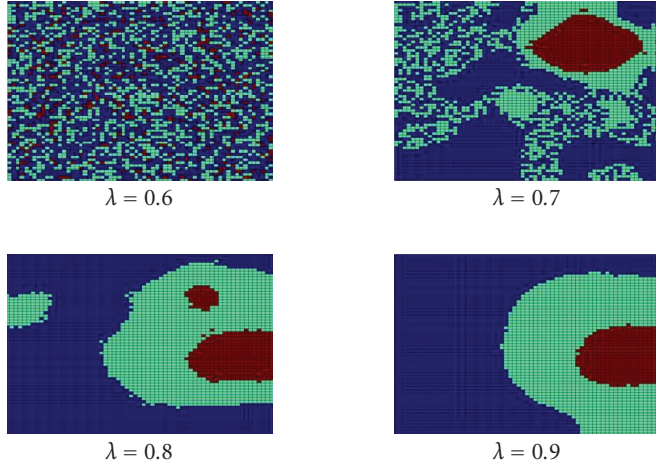


Figure 5.1. Asymptotic agent's distribution for different values of  $\lambda$  in the  $64 \times 64$  lattice. Here  $I(A^*) \approx 0.25$  and  $\lambda_c \approx 0.6$ .

the asymptotic distributions of agents  $A^*$ , obtained from the same initial condition  $A^0$  by using 4 different values of  $\lambda$ . Note how the asymptotic distribution acquires a more regular structure as we increase  $\lambda$ .

In order to determine  $\lambda_c$ , for a given initial agents' distribution  $A^0$ , we compute the evolution of the biorthogonal decomposition entropy  $H_{\text{BO}}(A^t)$ , considering increasing values of  $\lambda$ . If  $\lambda$  is small,  $H_{\text{BO}}(A^t)$  remains practically constant along the evolution, while for sufficiently large values of  $\lambda$ , this entropy undergoes a monotonous decreasing until a definite time that we call segregation time, at which it attains its limiting value. We illustrate this in Figure 5.2, where we show that  $H_{\text{BO}}(A^t)$  for  $\lambda < \lambda_c$  and  $\lambda > \lambda_c$ . Hence, the segregation time may be considered infinite for small values of  $\lambda$ , and taking finite values for  $\lambda \geq \lambda_c$ . We determine  $\lambda_c$  corresponding to an initial agents' distribution  $A^0$ , by computing  $H_{\text{BO}}(A^t)$  for  $\lambda = \lambda^* - 0.05, \lambda^*, \dots, \lambda^* + 0.15$ , and taking the smallest of these values for which segregation time is smaller than the empirically determined convergence time. The time  $T$ , that an initial configuration  $n A^0$  needs to attain the asymptotic distribution  $A^*$ , is increased with both  $I(A^0)$  and  $\lambda$ . Nevertheless, for the  $64 \times 64$  lattice and  $\lambda < 1$ , this time never exceeded 1200 iterations in our simulations. For the  $128 \times 128$  lattice, this convergence time at  $\lambda_c$  was always smaller than 2000, and never exceeded 3200 for the other values of  $\lambda$ . The convergence time  $T$  appears to increase in proportion to  $n \log(n)$ , where  $n$  is the lattice size.

In Figure 5.3, we show the behavior of  $\lambda_c$  as the inequality index changes, for the regular family in the  $64 \times 64$  lattice, and we compare it to the behavior of our a priori estimate  $\lambda^*$ . All the computations presented here correspond to  $\alpha = 0.4$ , but the behavior we observed for other values of  $\alpha$  is qualitatively the same. In Figure 5.4, we display the same comparison for to the  $128 \times 128$  lattice. Since  $\lambda^*$  depends only on the proportions of

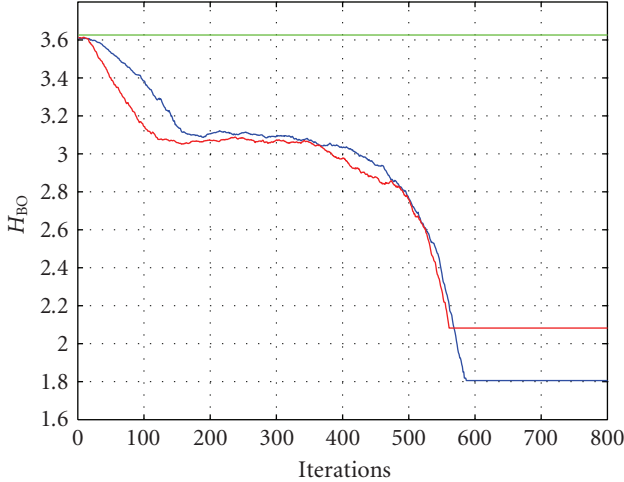


Figure 5.2. Evolution of the segregation index  $H_{BO}(A^t)$ . We show two experiments in the  $64 \times 64$  lattice, for an agents' distribution with inequality index  $I = 0.5$  and  $\lambda^* \approx 0.68$ . The green horizontal line corresponds to  $\lambda = 0.65$ , the blue line was computed with  $\lambda = 0.75$ , and the red was obtained using  $\lambda = 0.8$ .

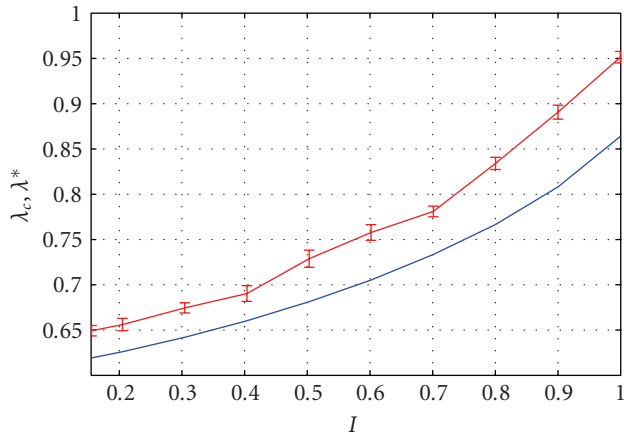


Figure 5.3.  $\lambda_c$  with its error bars shown in red as function of Theil's inequality index, and  $\lambda^*$  shown in blue as a function  $I$ . Both curves correspond to the regular family, with  $\alpha = 0.4$ , in the  $64 \times 64$  lattice.

rich, middle class and poor agents, it is lattice size independent. According to our numerical results, our a priori estimate is a reasonably tight lower bound for  $\lambda_c$ . Let us remark that the numerical value of  $\lambda_c$  slightly depends on the initial condition of the experiment, hence we plot the mean value of  $\lambda_c$  and the corresponding error bars.

For the family  $\mathcal{F}_{mp}$ , we show in Figures 5.5 and 5.6 the behavior of  $\lambda_c$  as a function of the inequality index, in the  $64 \times 64$  and  $128 \times 128$  lattices, respectively. We compare this to the behavior of our a priori estimate  $\lambda^*$ . Since  $\lambda_c$  slightly depends on the initial

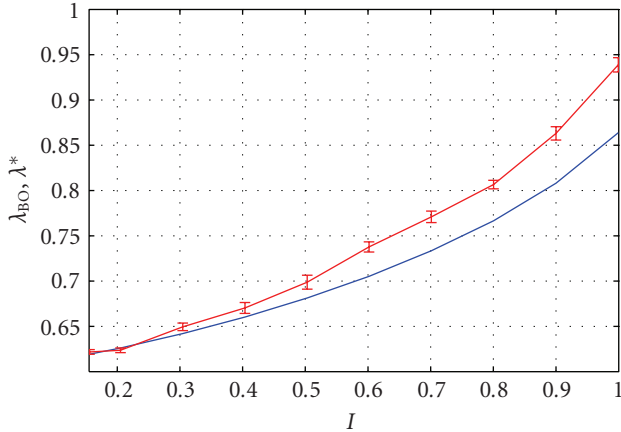


Figure 5.4.  $\lambda_c$  is shown in red, with its error bars, as function of Theil's index  $I$ .  $\lambda^*$  is shown in blue also as a function of  $I$ . Both curves correspond to the regular family, with  $\alpha = 0.4$ , in the  $128 \times 128$  lattice.

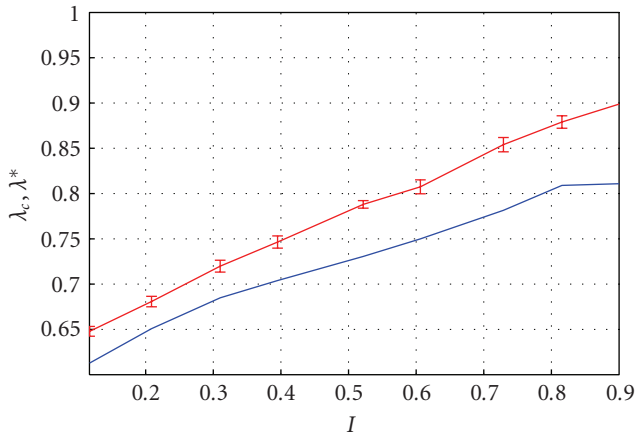


Figure 5.5.  $\lambda_c$  is shown in red, with its error bars, as a function of  $I$ .  $\lambda^*$  is shown in blue also as a function of Theil's inequality index  $I$ . Both curves correspond to the family  $\mathcal{F}_{mp}$  in the  $64 \times 64$  lattice.

condition, we show  $\lambda_c$  with the corresponding error bars. Once again,  $\lambda^*$  is a reasonably tight lower bound for the actual value of  $\lambda_c$ .

In Figures 5.7 and 5.8, we plot the segregation index  $S_{BO}$  as function of the inequality index, for the regular family in the  $64 \times 64$  and  $128 \times 128$  lattices, respectively. These are the inequality-segregation curves our model produces. We compare those curves to our a priori upper bound estimate  $S^* := \log(n/\sqrt{N_r})$  with  $n = 64$  and  $128$ , which we derived at the end of Section 4. In Figures 5.9 and 5.10, we plot the same data, corresponding to the family of most probable demographic scenarios. Our numerical results show that in the case of the regular family, our prediction holds for inequality indices in the interval  $0 \leq I \leq 0.5$ . For the family of the most probable demographic scenarios, the a priori upper

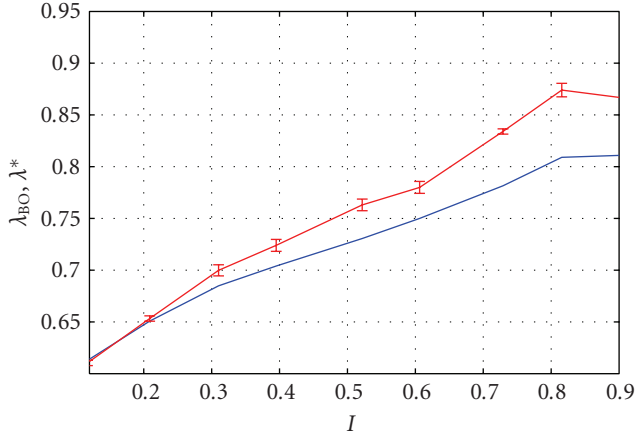


Figure 5.6.  $\lambda_c$  is shown in red, with its error bars, as a function of Theil's inequality index  $I$ .  $\lambda^*$  is shown in blue also as a function of  $I$ . Both curves correspond to the family  $\mathcal{F}_{\text{mp}}$  in the  $128 \times 128$  lattice.

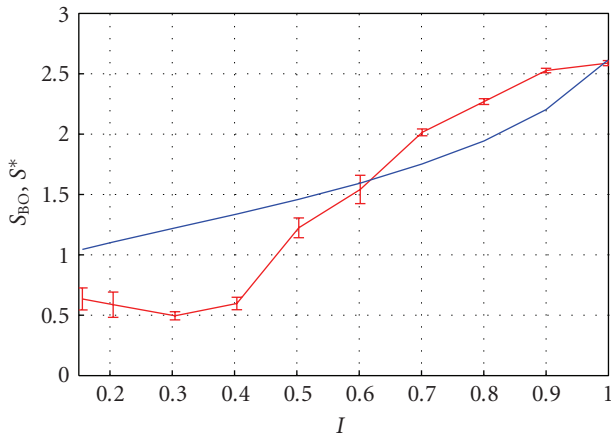


Figure 5.7. The segregation index  $S_{\text{BO}}$  is shown in red, with its error bars, as function of  $I$ .  $S^* = \log(64/\sqrt{N_r})$  is shown in blue also as a function of  $I$ . These inequality-segregation curves correspond to the  $\mathcal{F}_\alpha$  family, with  $\alpha = 0.40$ , in the  $64 \times 64$  lattice.

bound holds up to  $I = 0.7$ . The exact value of  $S_{\text{BO}}(A^*)$  depends on the initial condition  $A^0$ , therefore, we show its mean value with the corresponding error bars.

## 6. Discussion and conclusions

The model presented here provides a pattern formation mechanism which can be interpreted in terms of Massey's thesis. This mechanism takes into account two socioeconomic variables, namely the income inequality and the spatial distribution of individuals. The model yields a correlation between those two variables in a way which is consistent with

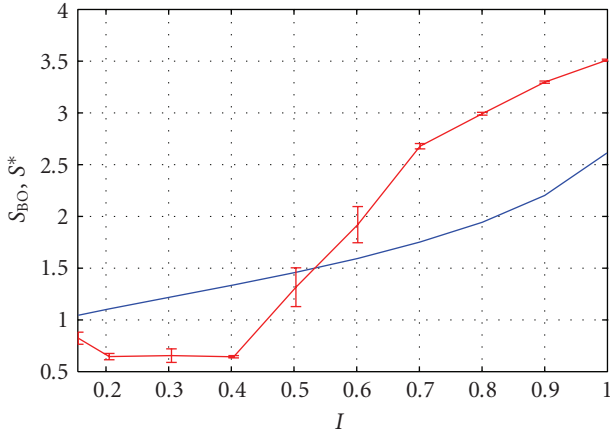


Figure 5.8. The inequality-segregation curve,  $S_{BO}$  is shown in red as function of  $I$ . Here the segregation index  $S_{BO}$  is plotted with its error bars.  $S^* = \log(128/\sqrt{N_r})$  is shown in blue also as a function of  $I$ . Both curves correspond to the  $\mathcal{F}_\alpha$  family, with  $\alpha = 0.40$ , in the  $128 \times 128$  lattice.

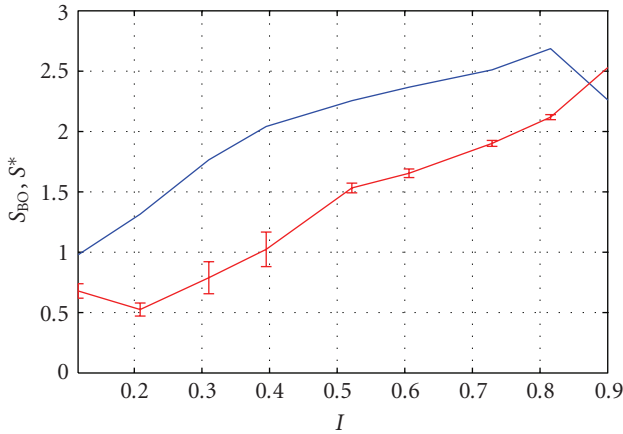


Figure 5.9. The segregation index  $S_{BO}$  is shown in red, with the respective error bars, as function of  $I$ .  $S^* = \log(64/\sqrt{N_r})$  is shown in blue as a function of Theil's inequality index  $I$ . Both curves correspond to the  $\mathcal{F}_{mp}$  family in the  $64 \times 64$  lattice.

the segregation-inequality curve proposed by Morrison. Following Schelling, we built our model upon simple rules governing householders' exchange location in a virtual city. We include a control parameter which we relate to the adjustments of the house prices during the evolution, in a way that segregation occurs only for large enough values of this parameter. With these simple features, we are able to produce spatial patterns whose degree of order grows with the income inequality of the virtual city.

From the point of view of social and economical theories, the mechanism behind the migration of agents and the price function may appear unrealistic, however, they were not arbitrarily designed. The agents exchange mechanism is inspired by Schelling's happiness

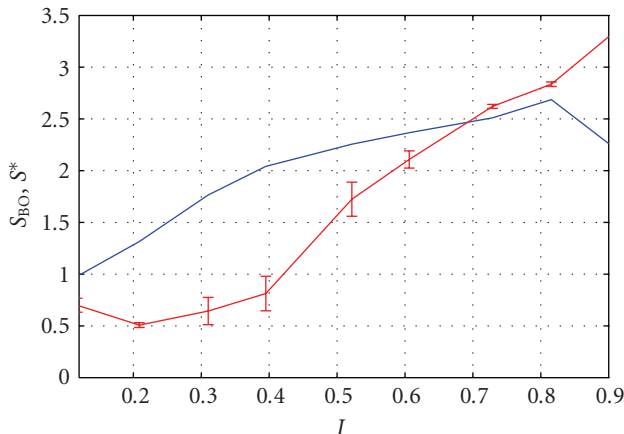


Figure 5.10. The segregation index  $S_{BO}$  is shown in red, with the respective error bars, as function of Theil's inequality index  $I$ .  $S^* = \log(128/\sqrt{N_r})$  is shown in blue also as a function  $I$ . Both curves correspond to the  $\mathcal{F}_{mp}$  family in the  $128 \times 128$  lattice.

function, while the house prices dynamics is similar to the one proposed by Portugali and Benenson. Instead of a sophisticated housing prices theory, we use simple interaction rules that we believe to constitute an acceptable first approximation to the actual housing prices dynamics.

Though the mechanism driving the migration of agents retains many of Schelling's ideas, it differs in the nature of the location exchange decision. In Schelling's original model, this decision is taken based on a satisfaction function that takes into account the number of neighbors of the same kind around a given agent. In our case, an agent decides to exchange its location according to the difference between its income and the price of its house. This mechanism is better suited for a model of a society where ethnic differences are less determinant than differences imposed by the income.

Concerning the indicators we use, Theil's index is a widely accepted inequality index, with the advantage that it is easy to compute and has a direct interpretation. Our segregation index, on the other hand, has never been used in this context. Besides this indicator, we previously tried other entropy-like measures of the degree of order in a spatial distribution, as well as some direct clustering measures. We chose the entropy of the biorthogonal decomposition because it is almost as easy to compute as Theil's index, and it has a natural interpretation as the information contents of a picture. We are convinced that other segregation measures commonly used in the sociological literature are not suited for our purposes, mainly because they suppose a previous knowledge of the spatial structure of the city. In our case, the organization of the urban space is a result only of the location exchange dynamics.

From the theoretical point of view, the model is interesting by its own. It exhibits an order-disorder phase transition via clustering from a very simple exchange mechanism. It also appears to present some finite-size scaling behavior which would be pertinent to further explore.

Summarizing, our model is built from a very simple location exchange rule, based on interaction between agents through an economic tension produced by the difference between the agents' economic capacity and the prices of the houses they occupy. It constitutes an alternative to Schelling's exchange mechanism including an extra degree of freedom, our parameter  $\lambda$ , which could have an economic interpretation. In this way, we obtain a mathematically tractable model which could be further modified in order to include more realistic features. In its current form, our model provides simple mechanism sufficient to produce spatial segregation in accordance to Massey's thesis: segregation is an increasing function of the inequality. More realistic reformulations of this model, which would include vacancies and agents queueing for a vacant locations, will be considered for further study.

## References

- [1] L. S. Bourne, "Urban structure and land use decisions," *Annals of the Association of American Geographers*, vol. 66, no. 4, pp. 531–547, 1976.
- [2] T. Duncan, *The Urban Mosaic: Towards a Theory of Residential Differentiation*, Cambridge University Press, Cambridge, UK, 1971.
- [3] J. R. Logan and H. L. Molotch, *Urban Fortunes: The Political Economy of Place*, University of California Press, Berkeley, Calif, USA, 1987.
- [4] A. R. Tickamyer, "Space matters! spatial inequality in future sociology," *Contemporary Sociology*, vol. 29, no. 6, pp. 805–813, 2000.
- [5] A. Wilson, *Complex Spatial Systems: The Modeling Foundations of Urban and Regional Analysis*, Pearson Education, England, UK, 2001.
- [6] D. S. Massey and N. A. Denton, "The dimensions of residential segregation," *Social Forces*, vol. 67, no. 2, pp. 281–315, 1988.
- [7] D. S. Massey, A. B. Gross, and M. L. Eggers, "Segregation, the concentration of poverty, and the life chances of individuals," *Social Science Research*, vol. 20, no. 4, pp. 397–420, 1991.
- [8] D. S. Massey, A. B. Gross, and K. Shibuya, "Migration, segregation, and the geographic concentration of poverty," *American Sociological Review*, vol. 59, no. 3, pp. 425–445, 1994.
- [9] N. R. Cloutier, "Urban residential segregation and black income," *The Review of Economics and Statistics*, vol. 64, no. 2, pp. 282–288, 1982.
- [10] P. A. Jargoswky, "Take the money and run: economic segregation in U.S. metropolitan areas," *American Sociological Review*, vol. 61, no. 6, pp. 984–998, 1996.
- [11] D. S. Massey, "Effects of socioeconomic factors on the residential segregation of blacks and Spanish Americans in U.S. urbanized areas," *American Sociological Review*, vol. 44, no. 6, pp. 1015–1022, 1979.
- [12] O. D. Duncan and B. Duncan, "A methodological analysis of segregation indexes," *American Sociological Review*, vol. 20, no. 2, pp. 210–217, 1955.
- [13] D. S. Massey, M. J. White, and V.-C. Phua, "The dimensions of segregation revisited," *Sociological Methods & Research*, vol. 25, no. 2, pp. 172–206, 1996.
- [14] I. Benenson, "Multi-agent simulations of residential dynamics in the city," *Computers, Environment and Urban Systems*, vol. 22, no. 1, pp. 25–42, 1998.
- [15] W. A. V. Clark, "Residential preferences and neighborhood racial segregation: a test of the Schelling segregation model," *Demography*, vol. 28, no. 1, pp. 1–19, 1991.
- [16] M. Fossett, "Ethnic preferences, social distance dynamics, and residential segregation: results from simulation analyses," in *The Annual Meetings of the American Sociological Association*, Chicago, Ill, USA, August 1999, <http://sociweb.tamu.edu/fossett/asa99mf.pdf>.

- [17] M. Fossett, “Racial preferences and racial residential segregation: findings from analyses using minimum segregation models,” Working Paper, Race and Ethnic Studies Institute, Texas A&M University, College Station, Tex, USA, August 2003, [http://sociweb.tamu.edu/faculty/fossett/paa2004\\_revised.pdf](http://sociweb.tamu.edu/faculty/fossett/paa2004_revised.pdf).
- [18] S. Lieberson and D. K. Carter, “A model for inferring the voluntary and involuntary causes of residential segregation,” *Demography*, vol. 19, no. 4, pp. 511–526, 1982.
- [19] D. S. Massey and N. A. Denton, “Spatial assimilation as a socioeconomic outcome,” *American Sociological Review*, vol. 50, no. 1, pp. 94–106, 1985.
- [20] D. S. Massey, “American apartheid: segregation and the making of the underclass,” *American Journal of Sociology*, vol. 96, no. 2, pp. 329–357, 1990.
- [21] I. Omer, “Demographic processes and ethnic residential segregation,” *Discrete Dynamics in Nature and Society*, vol. 3, no. 2–3, pp. 171–184, 1999.
- [22] D. Osullivan, J. M. Macgill, and C. Yu, “Agent-based residential segregation: a hierarchically structured spatial model,” in *Agent 2003 ‘Challenges in Social Simulation’*, University of Chicago and Argone National Laboratory, Chicago, Ill, USA, October 2003, [http://www.geog.psu.edu/people/osullivan/publications/conf/agent2003/Agent2003\\_Paper\\_Osullivan\\_online.pdf](http://www.geog.psu.edu/people/osullivan/publications/conf/agent2003/Agent2003_Paper_Osullivan_online.pdf).
- [23] J. Portugali, I. Benenson, and I. Omer, “Spatial cognitive dissonance and sociospatial emergence in a self-organizing city,” *Environment and Planning B: Planning and Design*, vol. 24, no. 2, pp. 263–285, 1997.
- [24] T. C. Schelling, “Models of segregation,” *The American Economic Review*, vol. 59, no. 2, pp. 488–493, 1969.
- [25] T. C. Schelling, “Dynamic models of segregation,” *Journal of Mathematical Sociology*, vol. 1, no. 2, pp. 143–186, 1971.
- [26] T. C. Schelling, *Micromotives and Macrobehavior*, W. W. Norton, New York, NY, USA, 1978.
- [27] J. Zhang, “A dynamic model of residential segregation,” *Journal of Mathematical Sociology*, vol. 28, no. 3, pp. 147–170, 2004.
- [28] P. S. Morrison, P. Callister, and J. Rigby, “The spatial separation of work-poor and work-rich households in New Zealand 1986–2001: an introduction to a research project,” School of Earth Sciences Research Report 17, Victoria University of Wellington, Wellington, New Zealand, April 2003.
- [29] K. Sznajd-Weron and R. Weron, “A simple model of price formation,” *International Journal of Modern Physics C*, vol. 13, no. 1, pp. 115–123, 2002.
- [30] D. Stauffer, “Monte Carlo simulations of Sznajd models,” *Journal of Artificial Societies and Social Simulation*, vol. 5, no. 1, 2002.
- [31] D. Stauffer, “The Sznajd model of consensus building with limited persuasion,” *International Journal of Modern Physics C*, vol. 13, no. 3, pp. 315–317, 2002.
- [32] D. Stauffer, “Sociophysics simulations II: opinion dynamics,” in *Proceedings of AIP Conference*, vol. 779, pp. 56–68, Granada, Spain, February 2005.
- [33] K. Sznajd-Weron, “Opinion evolution in closed community,” *International Journal of Modern Physics C*, vol. 11, no. 6, pp. 1157–1165, 2000.
- [34] S. Galam, “Minority opinion spreading in random geometry,” *The European Physical Journal B—Condensed Matter and Complex Systems*, vol. 25, no. 4, pp. 403–406, 2002.
- [35] S. Galam, “Modelling rumors: the no plane Pentagon French hoax case,” *Physica A: Statistical Mechanics and Its Applications*, vol. 320, pp. 571–580, 2003.
- [36] Y. Kabashima, “Propagating beliefs in spin-glass models,” *Journal of the Physical Society of Japan*, vol. 72, no. 7, pp. 1645–1649, 2003.
- [37] R. Axelrod, “The dissemination of culture: a model with local convergence and global polarization,” *Journal of Conflict Resolution*, vol. 41, no. 2, pp. 203–226, 1997.

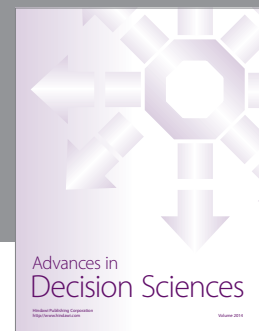
- [38] C. Castellano, M. Marsili, and A. Vespignani, “Nonequilibrium phase transition in a model for social influence,” *Physical Review Letters*, vol. 85, no. 16, pp. 3536–3539, 2000.
- [39] H. Meyer-Ortmanns, “Immigration, integration and ghetto formation,” *International Journal of Modern Physics C*, vol. 14, no. 3, pp. 311–320, 2003.
- [40] M. Pollicott and H. Weiss, “The dynamics of schelling-type segregation models and a nonlinear graph Laplacian variational problem,” *Advances in Applied Mathematics*, vol. 27, no. 1, pp. 17–40, 2001.
- [41] J. M. Sakoda, “The checkerboard model of social interaction,” *Journal of Mathematical Sociology*, vol. 1, no. 1, pp. 119–132, 1971.
- [42] W. Alonso, *Location and Land Use*, Harvard University Press, Cambridge, Mass, USA, 1964.
- [43] R. Benabou, “Workings of a city: location, education, and production,” *The Quarterly Journal of Economics*, vol. 108, no. 3, pp. 619–652, 1993.
- [44] G. Borjas, “Ethnicity, neighbourhood and human-capital externalities,” *American Economic Review*, vol. 85, no. 3, pp. 365–390, 1995.
- [45] D. S. Massey and M. J. Fischer, “How segregation concentrates poverty,” *Ethnic and Racial Studies*, vol. 23, no. 4, pp. 670–691, 2000.
- [46] J. Portugali, *Self-Organization and the City*, Springer, Berlin, Germany, 2000.
- [47] H. Theil, *Economic and Information Theory*, North Holland, Amsterdam, The Netherlands, 1967.
- [48] J. A. Dente, R. Vilela Mendes, A. Lambert, and R. Lima, “The bi-orthogonal decomposition in image processing: signal analysis and texture segmentation,” *Signal Processing: Image Communication*, vol. 8, no. 2, pp. 131–148, 1996.

Antonio Aguilera: Programa de Estudios Políticos e Internacionales, El Colegio de San Luis, A.C., Parque de Macul 155, Frac. Colinas del Parque, CP 78299 San Luis Potosí, SLP, Mexico  
*Email address:* aaguilera@colsan.edu.mx

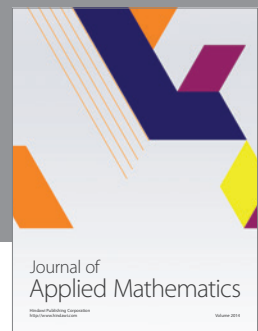
Edgardo Ugalde: Instituto de Física, Universidad Autónoma de San Luis Potosí, Av. Manuel Nava 6, Zona Universitaria, CP 78290 San Luis Potosí, SLP, Mexico  
*Email address:* ugalde@ifisica.uaslp.mx



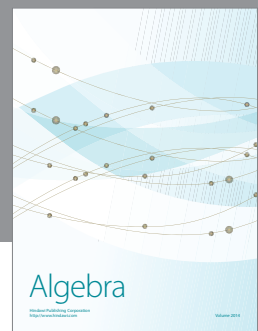
Advances in  
Operations Research



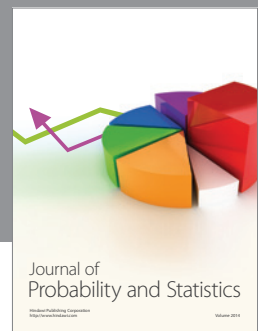
Advances in  
Decision Sciences



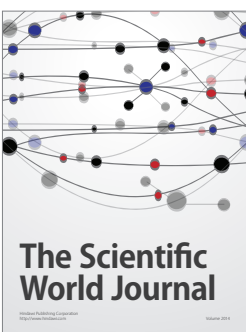
Journal of  
Applied Mathematics



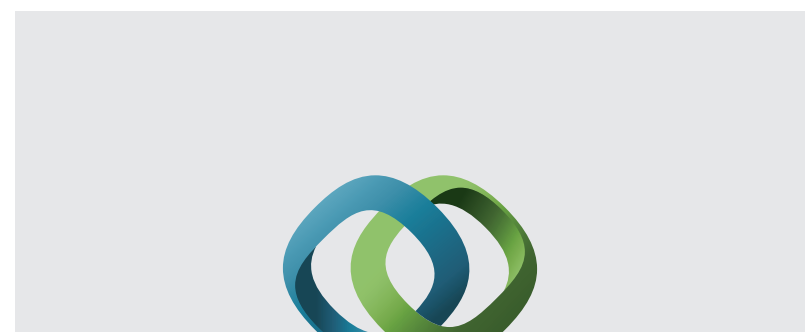
Algebra



Journal of  
Probability and Statistics

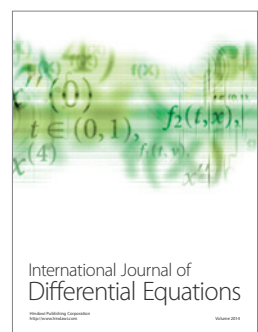


The Scientific  
World Journal



Hindawi

Submit your manuscripts at  
<http://www.hindawi.com>



International Journal of  
Differential Equations



International Journal of  
Combinatorics



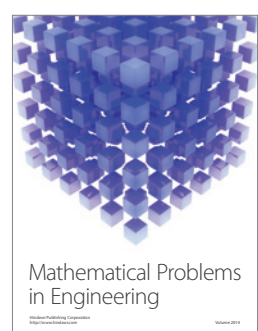
Advances in  
Mathematical Physics



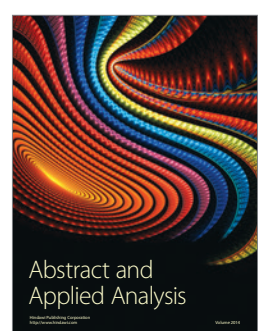
Journal of  
Complex Analysis



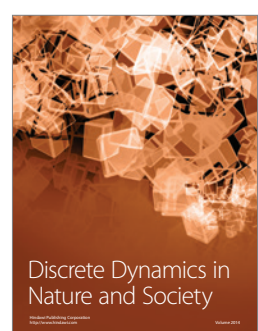
Journal of  
Mathematics



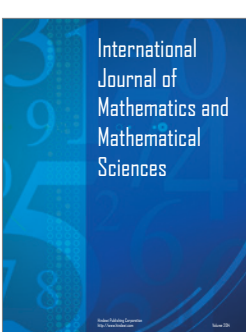
Mathematical Problems  
in Engineering



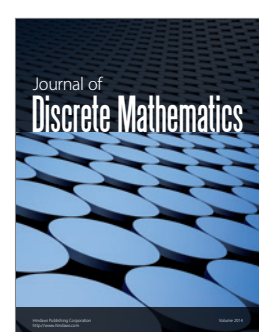
Abstract and  
Applied Analysis



Discrete Dynamics in  
Nature and Society



International  
Journal of  
Mathematics and  
Mathematical  
Sciences



Journal of  
Discrete Mathematics



Journal of  
Function Spaces



International Journal of  
Stochastic Analysis



Journal of  
Optimization